STUDIA UNIVERSITATIS BABEŞ-BOLYAI, CHEMIA, XLVIII, 2, 2003

CAPRA – A LEAPFROG RELATED MAP OPERATION

MIRCEA V. DIUDEA

Faculty of Chemistry and Chemical Engineering
Babes-Bolyai University, 400028 Cluj, Romania
diudea@chem.ubbcluj.ro

ABSTRACT. A map *M* is a combinatorial representation of a closed surface. Its corresponding graph can be either a periodic covering or an irregular one. Several operations on the map allow its transformation in tilings eventually of chemical interest. A new operation called “capra" is defined and exemplified. It is compared with the well known leapfrog and quadrupling transformations and its implications in the adjacency matrix eigenvalue spectra discussed.

INTRODUCTION

The discovery of fullerenes and related nanostructures has generated an explosion of research in theoretical and applied sciences. These new carbon allotropes show unusual properties (electronic, optical, mechanical, catalytic or capillarity), with no known analogy in nature. They are promising candidates for the development of nanodevices and super strong composites. Several books in this field have already been published.[1-5]

A fullerene is, according to a classical definition, an all-carbon molecule consisting entirely of pentagons (exactly 12) and hexagons (*N*/2-10). Non-classical fullerene extensions to include rings of other sizes have been considered.[6,7] Heterocyclic large cages have also been studied.[8]

A map *M* is a combinatorial representation of a closed surface.[9,10] The graph associated to the map is called regular if all its vertices have the same degree. Let us denote in a map: *v* - number of vertices, *e* - number of edges, *f* - number of faces and *d* - vertex degree. A subscript index will mark the corresponding parameters in the parent (zero) and (iteratively) transformed maps (1,2,..).

Recall the basic relations in a map:

$$\sum d v_d = 2e \qquad (1)$$

$$\sum s f_s = 2e \qquad (2)$$

where v_d and f_s are the number of vertices of degree *d* and number of *s*-gonal faces, respectively. The two relations are joined in the celebrated Euler[11] formula:

$$v - e + f = \chi(M) = 2(1-g) \qquad (3)$$

This work is dedicated to Prof. Dr. Patrick W. Fowler, School of Chemistry, University of Exeter, UK, for his pioneering research in the theoretical field of fullerenes and nanostructures.

with χ being the Euler *characteristic* and *g* the genus[12] of a graph (*e.g.*, *g* = 0 for a planar graph and 1 for a toroidal graph). Positive/negative χ values indicate positive/ negative curvature of a lattice. This formula is useful for checking the consistency of an assumed structure.

OPERATIONS ON MAPS

Several operations on maps are known and used for various purposes.

Stellation St of a face is achieved by adding a new vertex in its center and connecting it with each boundary vertex. It is also called a *capping* operation or (centered) *triangulation*.[9] When all the faces of a map are thus operated, it is referred to as an omnicapping operation. The resulting map shows the relations:

$$St(M): \quad v = v_0 + f_0 \,;\; e = 3e_0 \,;\; f = 2e_0 \qquad (4)$$

so that the Euler's relation holds.

Dualization Du of a map is built as follows: locate a point in the center of each face. Join two such points if their corresponding faces share a common edge. The transformed map is called the (Poincaré) *dual Du*(*M*). The vertices of *Du*(*M*) represent the faces of *M* and *vice-versa*.[9] Thus the following relations exist:

$$Du(M): \quad v = f_0 \,;\; e = e_0 \,;\; f = v_0 \qquad (5)$$

Dual of the dual recovers the original map: *Du*(*Du*(*M*)) = *M*.

Medial Me is an important operation of a map.[9,10,13] It is constructed as follows: put the new vertices as the midpoints of the original edges. Join two vertices if and only if the original edges span an angle. More exactly, the two edges must be incident and consecutive within a rotation path around their common vertex in the original map.

The medial graph is a subgraph of the line-graph.[12] In the line-graph each original vertex gives rise to a complete graph while in the medial graph only a cycle C_d (*i.e.*, a *d*-fold cycle, *d* being the vertex degree) is formed. The medial of a map is a 4-valent graph and *Me*(*M*) = *Me*(*Du*(*M*)). The transformed parameters are:

$$Me(M): \quad v = e_0 \,;\; e = 2e_0 \,;\; f = f_0 + v_0 \qquad (6)$$

The medial operation rotates parent *s*-gonal faces by π/s.

Truncation Tr is achieved by cutting of the neighborhood of each vertex by a plane close to the vertex, such that it intersects each edge incident to the vertex. Truncation is similar to the medial, with the main difference that each old edge will generate three new edges in the truncated map. The transformed parameters are:

$$Tr(M): \quad v = d_0 v_0 \,;\; e = 3e_0 \,;\; f = f_0 + v_0 \qquad (7)$$

Leapfrog Le is a composite operation[10,13-19] that can be written as:

$$Le(M) = Du(St(M)) = Tr(Du(M)) \qquad (8)$$

A sequence stellation-dualization rotates parent *s*-gonal faces by π/*s*. Note that the vertex degree in *Le*(*M*) is *always* 3, as a consequence of the involved triangulation. The transformed parameters are identical to those of *Tr*(*M*), eq. 7. Leapfrog operation is illustrated, for a square face, in Figure 1.

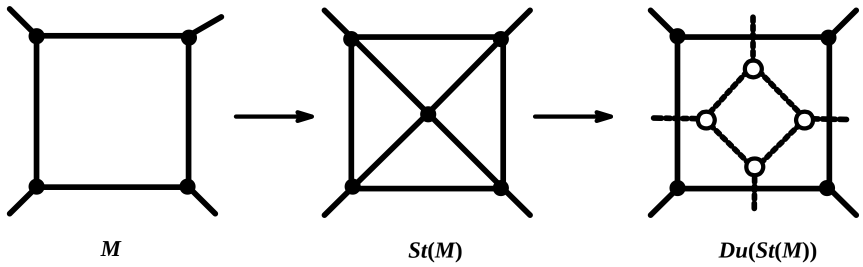

Figure 1. *Leapfrog of a square face of a trivalent map*

Note that a bounding polygon is formed around each original vertex. In the more frequent cases of tetra- and three-valent vertices, the bounding polygon is an octagon and a hexagon, respectively (Figure 2).

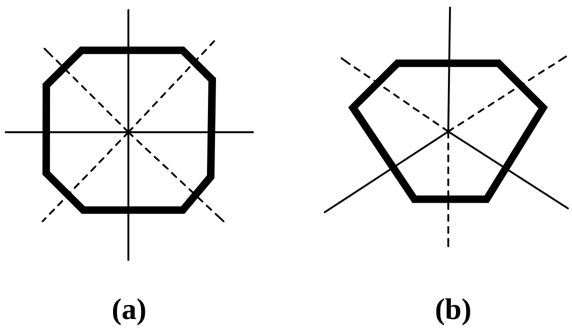

Figure 2. *Dualization of the omnicapped faces around a four-degree (a) and three-degree (b) vertex*

Leapfrog operation is exemplified in case of *M* = Dodecahedron (Figure 3).

Dodecahedron (C_{20})

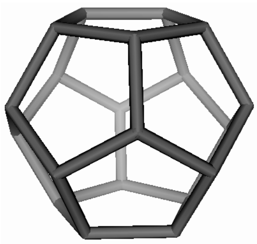

St(Dodecahedron)

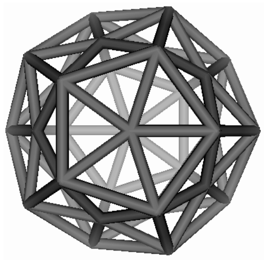

Icosahedron = *Du*(Dodecahedron)

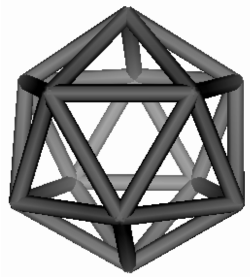

C_{60} = *Le*(Dodecahedron)

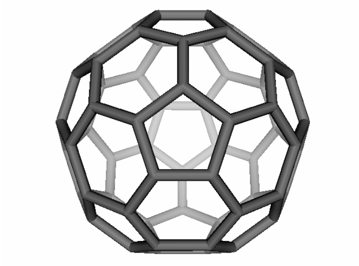

Figure 3. *Leapfrog operation of a trivalent cage*

Quadrupling Q is a transformation that preserves the initial orientation of all parent faces in the map.[13,18,20] It is also called the *chamfering* transformation.[21-23]

Q operation involves two π/s rotations, so that the initial orientation of the polygonal faces is conserved. Note that the quadrupling operation keeps the map vertices with their original valency. Clearly, the quadrupling transform of a four-valent map will not be anymore a regular graph.

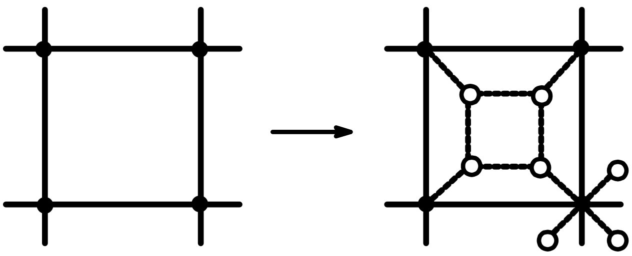

Figure 4. *Quadrupling a square face of a four-valent map*.

The transformed parameters are:[13,18]

$$Q(M): \quad v = (d_0 + 1)v_0 \; ; \; e = 4e_0 \; ; \; f = f_0 + e_0 \qquad (9)$$

Q may be written as a composite operation:

$$Q(M) = Du(Str(Me(M))) \quad (10)$$

where *Str* is a “reduced" *St*, with the meaning the triangles (*e.g*., those resulting by the medial operation) will not further be triangulated. This sequence of simple operations works well in trivalent maps *M* with no triangles.

The leapfrog and quadrupling operations can be used to get *isolate pentagons* in spherical fullerenes.[20]

Dual of the stellation of a medial Dsm is related to the *Q* operation, differing by the inclusion of the classical stellation in its sequence:

$$Dsm(M) = Du(St(Me(M))) = Le(Me(M))) \quad (11)$$

It is just the leapfrog of the medial and works well in four-valent square maps (Figure 5), thus completing each other with *Q*. The operation was useful in the decomposition of the chamfering operation.

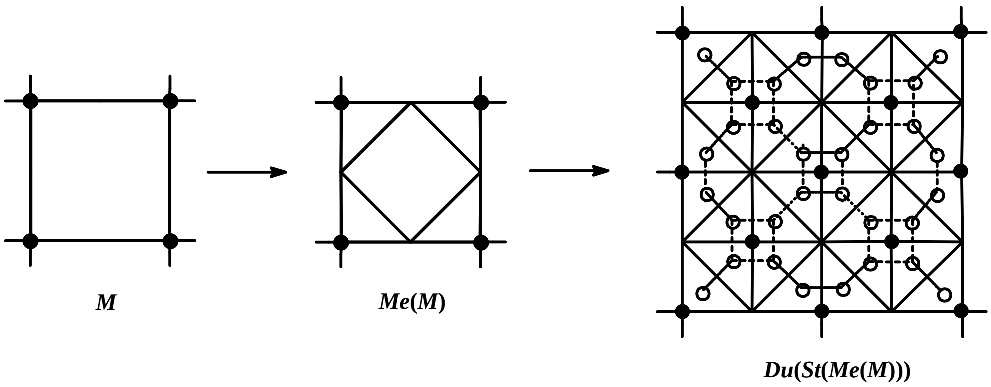

Figure 5. *Dual of the stellation of a medial Dsm transformation of a square four-valent map.*

It rotates the parent *s*-gonal faces by an even number of π/s, so that the original mutual orientation of edges-faces by *Dsm* is preserved. The transformed parameters are:[12,17]

$$Dsm\ (M):\ \ v = 2d_0 v_0 = 4e_0\,;\ \ e = 6e_0\,;\ \ f = f_0 + e_0 + v_0 \quad (12)$$

This operation, applied to square tiled tori, provided a [4, 8] covering with a multiplication ratio of 8.[13,18]

CAPRA OPERATION

Capra (the goat) is the Romanian corresponding of the *leapfrog* English children game. This name originates in a suggestion of A. T. Balaban about the *Le* operation. Thus, we call the herein proposed operation Capra *Ca*, which is defined as follows: put two points of degree two on each edge of the map (operation called *E2* in ref.[15]). Put a vertex in the center of each face of M and make (1, 4) connections, starting with a two-valent vertex. This operation we call *pentangulation Pe*, by analogy to the triangulation (see above). The last simple operation is a (reduced) truncation and thus:

$$Ca(M) = Trr(Pe(E2(M))) \quad (13)$$

It rotates the parent s-gonal faces by $\pi/2s$. The sequence above discussed is illustrated in Figure 6.

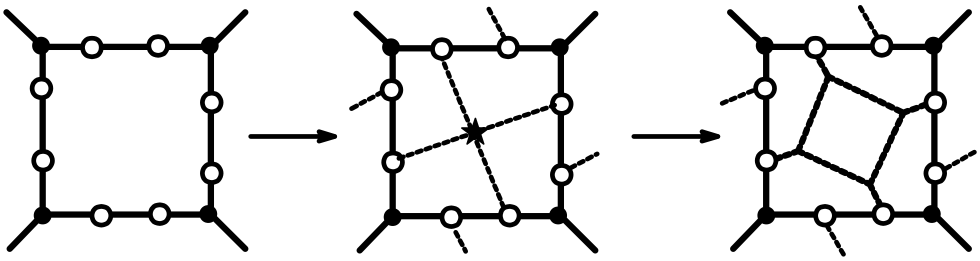

Figure 6. *Capra as a sequence of elementary operations.*

Ca-operation insulates each parent face by its own hexagons, in the opposite to *Le* and *Q*, in which two parent faces share one hexagon. It is illustrated Figure 7, for the cube.

Figure 8 illustrates the capra transformed of two other Platonic objects. Observe the clear difference between the regular trivalent lattice of C_{140} (*Ca*(Dodecahedron)) and that of C_{132} (*Ca*(Icosahedron)) which is an irregular net. It is due to the original five-valent vertices, preserved by *Ca*-operation (just as in case of *Q*) and dispersed among the newly introduced trivalent ones. In this last case, the triangles induce a strong positive curvature of the cage surface.

The transformed parameters are:

$$Ca(M): \quad v = (2d_0 + 1)v_0 = v_0 + 2e_0 + s_0 f_0 ; \; e = 3e_0 + 2s_0 f_0 ; \; f = (s_0 + 1) f_0 \quad (14)$$

In case of a trivalent regular *M* the vertex multiplication ratio is 7. Clearly, maps/graphs of degree other than 3 will not be regular anymore (see Figure 8).

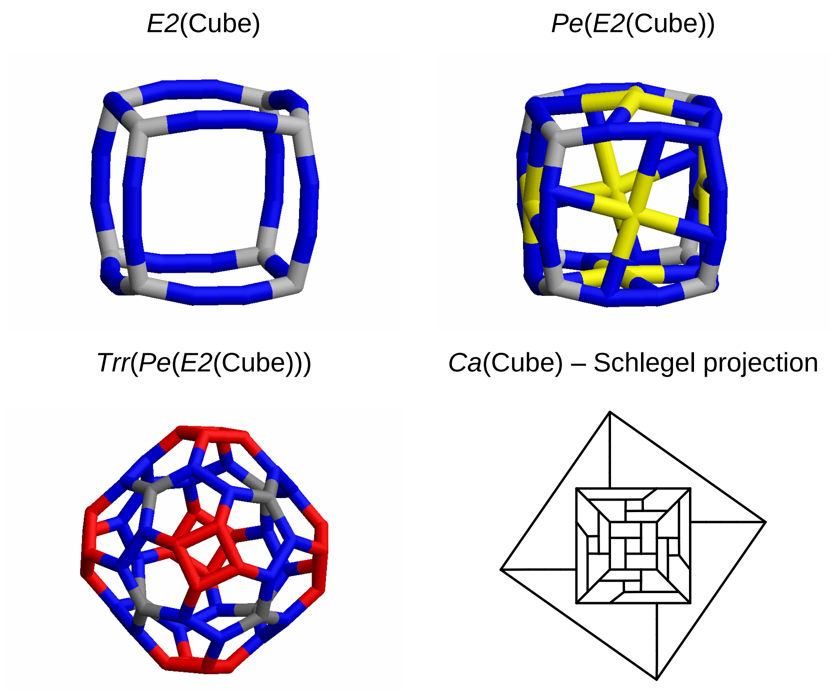

Figure 7. *Ca-operation in Cube and its Schlegel version*

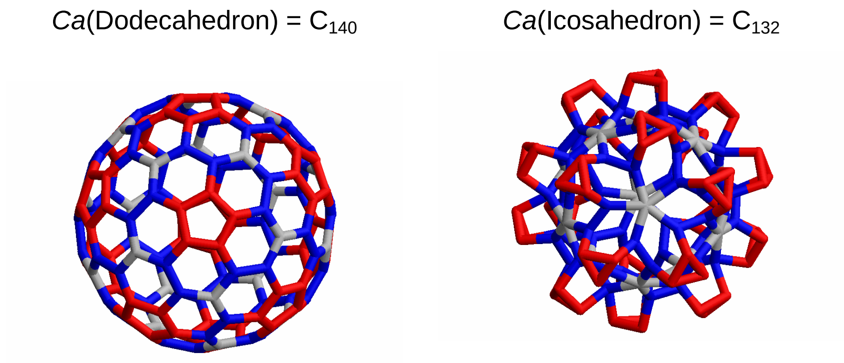

Figure 8. *Ca-operation in a trivalent- and a pentavalent-cage, respectively.*

A case apart is the open nanotubes (*g* changes from 0 (cylinder) to 1 (tube), by opening): Tuz[*c*,*n*] (a "zig-zag" (*c*/2,0) tube)[24] and Tua[*c*,*n*] (an "armchair" (*c*/2,*c*/2) tube), where *c* is the number of atoms in a cross-section while *n* is the number of cross-sections along the tube. The constitutive parameters for the tubes and Ca-transformed objects are given below:

Tuz[*c*,*n*] $v_0 = cn$ $\quad v = v_0 + 2e_0 + 6f_0 = 7v_0 - 4c$ (15)

$e_0 = cn + (c/2)(n-1) = v_0 + (v_0 - c)/2 \quad e = (21v_0 - 15c)/2$

$f_0 = (c/2)(n-1) = (v_0 - c)/2 \quad f = 7(v_0 - c)/2$

Tua[*c*,*n*] $v_0 = cn$ $\quad v = 7v_0 - 8c$ (16)

$e_0 = v_0 + v_0/2 - c \quad e = 21v_0/2 - 15c$

$f_0 = v_0/2 - c \quad f = 7v_0/2 - 7c$

When the pentangulation starts with the second point of degree 2, the result of Ca operation is the enantiomeric pair of the object built up by the first point procedure. Thus, (*CaS*(*M*) : *CaR*(*M*)) represent a “racemic" pair, in the *sinister-rectus* chemical terms. All the non-specified *Ca*-transforms are *CaS*(*M*). Figure 9 illustrates such a pair derived from the TUZ[8,3].

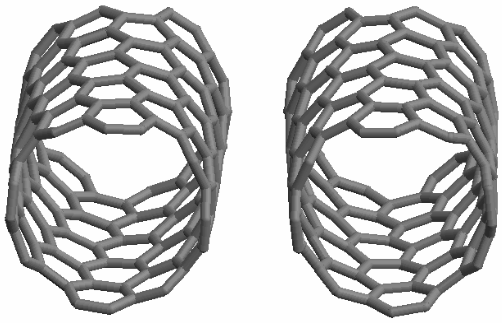

Figure 9. *A “racemic" pair of Ca-transformed TUZ[8,3]*

STRUCTURES WITH NEGATIVE CURVATURE

There exist natural materials, like zeolites, that show low density[25,26] coming from their constitutive micro pores. These pores can be simulated, *e.g.*, by structures tessellated entirely by heptagons (*e.g.*, the Klein tessellation) embedded into infinite periodic surfaces of negative curvature of genus >1.[23,27-29]

Capra transformed cages are easily transformed into all-heptagonal nets by the *E1* operation (*i.e*., insertion of one two-valent vertex) applied to every edge resulted in the truncation step. Figure 9 illustrates this transformation in cube.

A new *Ca*-operation on the object in Figure 10, $Ca(Ca(\text{Cube})_{[7]}) = Ca_2(\text{Cube})_{[7]}$, will result in a more relaxed structure, illustrated as embeddings in the periodic surfaces of negative curvature, in 2D and 3D, in Figure 11.

Ca(Cube)$_{[7]}$ *Ca*(Cube)$_{[7]}$ (optimized)

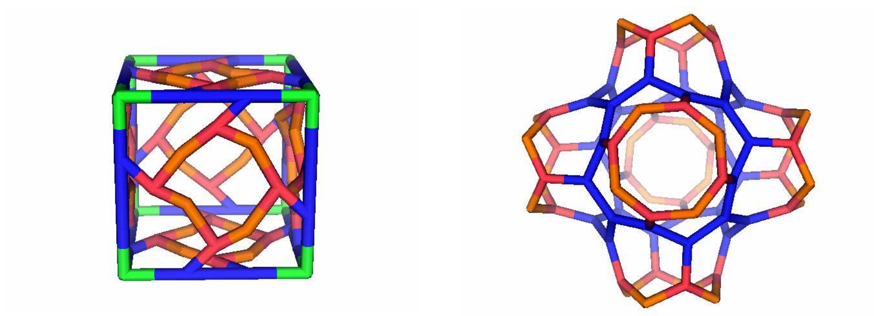

Figure 10. ***E1*** *operation in Cube*

The iterative application of *Ca* needs some modifications of eq. (14). In this respect, $Ca_n(M)$ will denote the n^{th} iteration while $Ca_n(M)_{[7]}$ the iteration made on the $Ca(M)_{[7]}$ (*i.e*., the all heptagonal cage of negative curvature). Relations (1) and (2) are re-written as: $2e_0 = d_0 v_0 = s_0 f_0$. The transformed parameters for the iterative *Ca* are given in Table 1.

Ca_2(Cube)$_{[7]}$, P2D Ca_2(Cube)$_{[7]}$, P3D

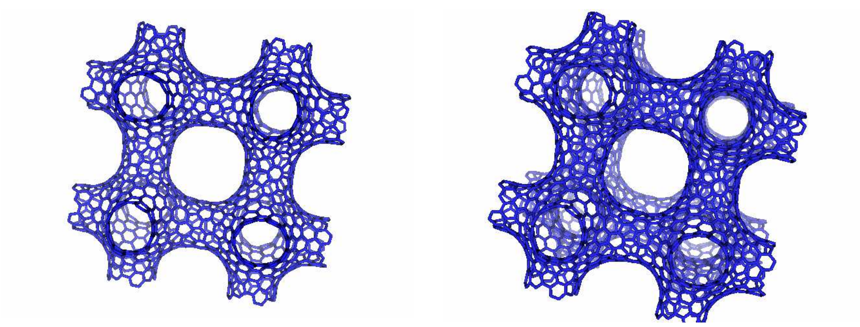

Figure 11*. Periodic surfaces of negative curvature, in 2D and 3D, respectively*

Note that, in case of the cube, the relation (20') is equivalent to (15), meaning $Ca_2(Cube)_{[7]}$ is equivalent with three interlacing *Tuz* nanotubes, following the rectangular 3D coordinates.

The [7] tiling embedded in the dodecahedron leads, after appropriate capping, to the celebrate "phantasmagoric" $_{[260]}$Fullerene of Fowler[30] (Figure 12).

Twice *Ca*-operation applied on both the primary *Ca*-transformed cage and [7] tiling is illustrated in Figure 13, for the tetrahedron. Observe the two extremes: positive and negative curvatures, respectively, of the lattices originating in the same parent cage.

A sequence of *CaS,CaR* will provide non-twisted objects. More about this subject will be presented in a future paper.

Table 1.

The transformed parameters for the iterative *Ca* operation

	Operation	Parameter	eq
1	$Ca(M)$	$v_1 = (2d_0 + 1)v_0 = v_0 + 2e_0 + s_0 f_0 = v_0 + 4e_0$ $e_1 = 7e_0$ $f_1 = (s_0 + 1) f_0 = f_0 + 2e_0$	(17)
2	$Ca(M)_{[7]}$	$v_{1[7]} = v_1 + s_0 f_0 = v_0 + 6e_0$ $e_{1[7]} = 9e_0$ $f_{1[7]} = f_1 - f_0 = 2e_0$	(18)
3	$Ca_2(M)$	$v_2 = v_1 + 2e_1 + s_1 f_1 = v_1 + 2e_1 + [6(s_0 f_0) + s_0 f_0]$ $= v_0 + 32e_0$ $e_2 = 7^2 \cdot e_0$ $f_2 = (s_1 + 1) f_1 = f_0 + 16e_0$ $v_2 = 7^2 \cdot v_0 \ ; d_0 = 3$	(19) (19')
4	$Ca_2(M)_{[7]}$	$v_{2[7]} = v_{1[7]} + 2e_{1[7]} + 7 f_{1[7]} = v_0 + 38e_0$ $e_{2[7]} = 3v_0 + 108e_0$ $f_{2[7]} = (7 + 1) f_{1[7]} = 16e_0$ $v_{2[7]} = 7v_{1[7]} - 3(4c) \ ; M = Cube$	(20) (20')
5	$Ca_n(M)$	$v_n = 8v_{n-1} - 7v_{n-2} \ ; n \ge 2; d_0 > 3$ $v_n = 7^n \cdot v_0 \ ; d_0 = 3$ $e_n = 7^n \cdot e_0 = 7^n \cdot 3v_0 / 2$ $f_n = f_0 + (7^n - 1) \cdot v_0 / 2$	(21) (21') (21'') (21''')

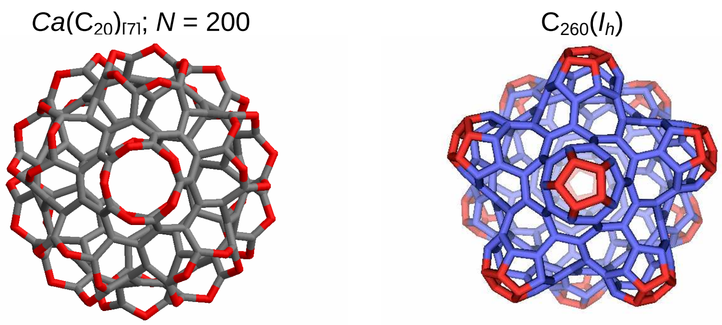

Figure 12. *Capping the [7] tiling of Dodecahedron results in the all [5, 7] C_{260} cage of icosahedral symmetry*

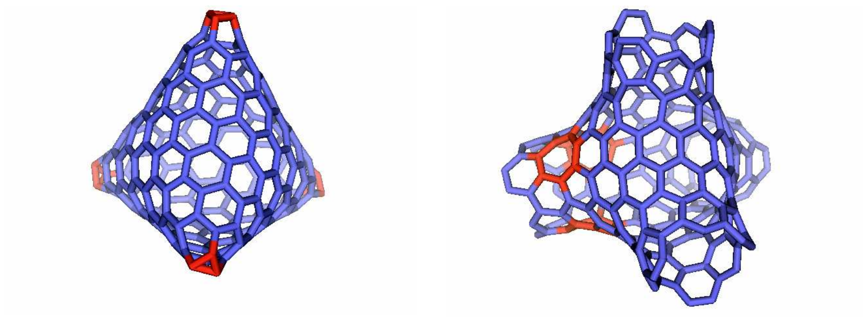

Figure 13. *Two extremes: positive and negative curvatures, respectively, of the lattices coming, by Ca, from Tetrahedron*

The genus of the $Ca(M)_{[7]}$ objects is calculable as follows:

$$\chi(M)_{[7]} = v_{1[7]} - e_{1[7]} + f_{1[7]} = 2 - 2g = v_0 - e_0 \quad (22)$$

$$g = (e_0 - v_0 + 2)/2 = f_0/2 \quad (23)$$

Relation (23) comes from the spherical character of the parent polyhedron, for which $v_0 - e_0 + f_0 = 2$. Clearly, lattices with $g > 1$ will have negative $\chi(M)_{[7]}$ and consequently negative curvature. For the five Platonic solids, the genus of the corresponding $Ca(M)_{[7]}$ is: 2 (Tetrahedron); 3 (Cube); 4 (Octahedron); 6 (Dodecahedron) and 10 (Icosahedron).

SPECTRAL PROPERTIES INVOLVING *Ca* OPERATION

In simple Hückel theory,[32] the energy of the i^{th} π-molecular orbital $E_i = \alpha + \lambda_i \beta$ is calculated on the grounds of the adjacency matrix associated to the molecular hydrogen depleted graph.

The π-electronic shells of neutral fullerenes are classified, function of their eigenvalue spectra, as:[31] (i) *properly closed*, PC, when $\lambda_{N/2} > 0 \geq \lambda_{N/2+1}$; (ii) *pseudo-closed*, PSC, in case $\lambda_{N/2} > \lambda_{N/2+1} > 0$; (iii) *meta-closed*, MC, with $0 \geq \lambda_{N/2} > \lambda_{N/2+1}$ and (iv) *open*, OP, when the $N/2^{th}$ (HOMO) and $N/2+1^{th}$ (LUMO) molecular orbitals are degenerate, $\lambda_{N/2} = \lambda_{N/2+1}$. The gap is taken as the absolute value of the difference $E_{(HOMO)}$ - $E_{(LUMO)}$. In nanotubes and tori, an open shell involving degenerate frontier orbitals: $HOMO_{-1}$, HOMO, LUMO and $LUMO_{+1}$ is called metallic M.

Ca-operation, applied on a finite structure, leaves unchanged its π-electronic shells. There exist exceptions, the most notably being the transformed *Ca*(Tuz/a[*c*,*n*]) of nanotubes (for symbols see ref. 33) which all have PC shell disregarding the character of their parent shell. Table 2 lists some examples in nanotubes and tori.

In the opposite, *Le* provides PC shell in fullerenes[15,34] and M shell in tori.[34] The other classical operation *Q* is, however, closer to *Ca*, both as construction and spectral aspects.

Interesting results are obtained in the Platonic polyhedra and their *Ca*-transforms (Table 3). The twice $Ca(M)_{[7]}$ would be low energy forms of carbon,[28,29] with exceeding electrons (see the last column in Table 3) in some degenerate antibonding orbitals. It is predicted to be electron-donating structures which stabilize as cations. No major modifications appear, in the spectrum of such objects, when $CaS(CaS(M)_{[7]})$ is changed by $CaR(CaS(M)_{[7]})$, see Table 3. Details will be given in a future paper.

Calculations of eigenvalues and map operations were made by TopoCluj 2.0 and CageVersatile 1.1 original softwares.[35,36]

Table 2.

Spectral data of nanotubes Tuz/a[*c*,*n*] and tori Z/A[*c*,*n*] and their *Ca*-transforms

	Structure	*N*	$HOMO_{-1}$	HOMO	LUMO	$LUMO_{+1}$	Gap	Shell
1	Tuz[8,4]	32	0.705	0	0	-0.705	0	OP
2	*Ca*(Tuz[8,4])	192	0.273	**0.017**	**-0.017**	-0.273	0.034	**PC**
3	Tuz[10,4]	40	0.095	0.095	-0.095	-0.095	0.190	PC
4	*Ca*(Tuz[10,4])	240	0.064	**0.064**	**-0.064**	-0.064	0.129	**PC**
5	Tua[4,8]	**32**	0.532	0	0	-0.532	0	OP
6	*Ca*(Tua[4,8])	192	0.265	**0.024**	**-0.024**	-0.265	0.048	**PC**
7	Tua[4,10]	**40**	0.310	0.169	-0.169	-0.310	0.338	PC
8	*Ca*(Tua[4,10])	248	0.132	**0.095**	**-0.095**	-0.132	0.189	**PC**
9	Z[8,10]	**80**	0.414	0.414	-0.414	-0.414	0.828	PC
10	*Ca*(Z[8,10])	560	0.169	0.169	-0.169	-0.169	0.337	PC
11	A[8,12]	**96**	0	0	0	0	0	M
12	*Ca*(A[8,12])	**672**	0	0	0	0	0	M

Table 3.

Spectral data of the Platonic polyhedra and their *Ca*-transforms

	Structure	$HOMO_{-1}$	HOMO	LUMO	$LUMO_{+1}$	Gap	Shell	Ex. *e*
1	*M* = Tetrahedron	3	**-1**	**-1**	-1	0	OP	
	$Ca(M)_{[7]}$	0.154	**0.154**	**0.154**	-0.614	0	OP	
	$CaS(CaS(M)_{[7]})$	-0.005	**-0.005**	**-0.005**	-0.306	0	OP	4
	$CaR(CaS(M)_{[7]})$	-0.010	**-0.010**	**-0.010**	-0.325	0	OP	4
2	*M* = Cube	1	1	-1	-1	2	PC	
	$Ca(M)_{[7]}$	0	0	0	-0.188	0	OP	
	$CaS(CaS(M)_{[7]})$	-0.010	**-0.010**	**-0.127**	-0.127	0.117	MC	6
	$CaR(CaS(M)_{[7]})$	-0.004	**-0.004**	**-0.141**	-0.141	0.137	MC	6

	Structure	$HOMO_{-1}$	HOMO	LUMO	$LUMO_{+1}$	Gap	Shell	Ex. *e*
3	*M* = Dodecahedron	1	**0**	**0**	0	0	OP	
	Ca(*M*)$_{[7]}$	0	**0**	**0**	-0.165	0	OP	
	CaS(*CaS*(*M*)$_{[7]}$)	-0.069	**-0.069**	**-0.069**	-0.131	0	OP	6
	CaR(*CaS*(*M*)$_{[7]}$)	-0.070	**-0.070**	**-0.070**	-0.138	0	OP	6
4	*M* = Octahedron	0	**0**	**0**	-2	0	OP	
	Ca(*M*)$_{[7]}$	0.222	**0**	**0**	0	0	OP	
	CaS(*CaS*(*M*)$_{[7]}$)	0.008	**-0.044**	**-0.044**	-0.044	0	OP	2
	CaR(*CaS*(*M*)$_{[7]}$)	0.021	**-0.058**	**-0.058**	-0.058	0	OP	2
5	*M* = Icosahedron	-1	**-1**	**-1**	-1	0	OP	
	Ca(*M*)$_{[7]}$	0.101	**0.101**	**0.101**	0.101	0	OP	
	CaS(*CaS*(*M*)$_{[7]}$)	-0.022	**-0.022**	**-0.022**	-0.022	0	OP	6
	CaR(*CaS*(*M*)$_{[7]}$)	-0.029	**-0.029**	**-0.029**	-0.029	0	OP	6

CONCLUSIONS

A new operation on maps, called *Capra Ca*, was proposed and discussed in comparison with the well-known leapfrog *Le* and quadrupling *Q* operations. Note that the Goldberg[37,38] relation: $m = (a^2 + ab + b^2); a \geq b; a + b > 0$ predicts our operation in the series: *Le:* (1, 1), *m* = 3; *Q:* (2, 0), *m* = 4 and *Ca:* (2, 1), *m* = 7.

Ca-operation insulates each parent face by its own hexagons (*i.e.*, coronene-like substructures), in contrast to *Le* and *Q*. The transformed constitutive parameters were given.

The utility of this operation is in building of large cages that preserve the symmetry and spectral properties of the parent structures and in extremely facile access to several constructions with negative curvature.

Clearly, many other authors have used such a transformation but no paper, in our best knowledge, has been devoted so far.

Acknowledgements. This paper was supported by the Romanian CNCSIS GRANT 2003.

REFERENCES

1. K. Tanaka, T. Yamabe, and K. Fukui, *The science and technology of carbon nanotues*, Elsevier, 1999.
2. M. Endo, S. Iijima and M. S. Dresselhaus, *Carbon Nanotubes*, Pergamon, 1996.
3. M. S. Dresselhaus, G. Dresselhaus, and P. C. Eklund, *Science of fullerenes and carbon nanotubes*, Acad. Press, San Diego, 1996.
4. Taylor, R., Ed., *The chemistry of fullerenes*, World Scientific: Singapore, 1995.
5. P. W. Fowler and D. E. Manolopolous, *An atlas of fullerenes*, Oxford University Press, Oxford, U.K., 1995.
6. Y. D. Gao and W. C. Herndon, *J. Amer. Chem. Soc*., **1993**, *115*, 8459.
7. P. W. Fowler, T. Heine, D. E. Manolopoulos, D. Mitchell, G. Orlandini, R. Schmidt, G. Seiferth and F. Zerbetto, *J. Phys. Chem.*, **1996**, *100*, 6984.

8. A. Müller, P. Kögerler, and Ch. Kuhlmann, *J. Chem. Soc*., *Chem. Commun*., **1999**, 1347-1358.
9. T. Pisanski, and M. Randić, in *Geometry at Work*, M. A. A. Notes, **2000**, *53*, 174-194.
10. P. W. Fowler and T. Pisanski, *J. Chem. Soc. Faraday Trans*. **1994**, *90*, 2865-2871.
11. L. Euler, *Comment*. *Acad. Sci. I. Petropolitanae*, ***1736***, *8*, 128-140
12. F. Harary, *Graph Theory*. Addison-Wesley, Reading, MA, **1969**.
13. M. V. Diudea, and P. E. John, *Commun. Math. Comput. Chem*. (*MATCH*), **2001**, *44* 103-116.
14. P. W. Fowler, *Phys. Lett*., **1986**, *131*, 444.
15. P. W. Fowler and J. I. Steer, *J. Chem. Soc*., *Chem. Commun*., **1987**, 1403-1405.
16. P. W. Fowler and K.M.Rogers, *J. Chem. Soc*., *Faraday Trans*., **1998,** *94***,** 1019-1027.
17. P. W. Fowler and K.M.Rogers, *J. Chem. Soc*., *Faraday Trans*., **1998,** *94***,** 2509-2514.
18. M. V. Diudea, P. E. John, A. Graovac, M. Primorac, and T. Pisanski, *Croat. Chem. Acta*, **2003**, *76*, 153-159.
19. G. Brinkmann, P. W. Fowler, and M. Yoshida, *MATCH Commun. Math. Comput. Chem.*, **1998**, *38*, 7-17.
20. P. W. Fowler, J. E. Cremona, and J. I. Steer, *Theor. Chim. Acta*, **1988**, *73*, 1.
21. A. Deza, M. Deza and V. P. Grishukhin, *Discrete Math*., ***1998***, *192*, 41-80.
22. M. Goldberg, *Tôhoku Math. J*., **1934**, *40*, 226-236.
23. A. Ceulemans, R.B. King, S. A. Bovin, K. M. Rogers, A Troisi, and P. W. Fowler, *J. Math. Chem.*, **1999**, *26*, 101-123.
24. A. L. Ivanovskii, *Russ. Chem. Rev*., **1999**, *68*, 103-118.
25. R. B. King, *J. Phys*. *Chem*., **1996**, *100*, 15096-15104.
26. R. B. King, *J. Chem*. *Inf*. *Comput*. *Sci*., **1998**, *38*, 180-188.
27. R. B. King, *Croat*. *Chem*. *Acta*, **2002**, *75*, 447-473.
28. M. O'Keeffe, G. B. Adams and O. F. Sankey, *Phys*. *Rev*. *Lett*., **1992**, *68*, 2325-2328.
29. T. Lenosky, X. Gonze, M. Teter and V. Elser, *Nature*, **1992**, *355*, 333-335.
30. A. Dress and G. Brinkmann, *MATCH- Commun. Math. Comput. Chem*., **1996**, *33*, 87-100.
31. P. W. Fowler and T. Pisanski, *J. Chem. Soc*., *Faraday Trans*., **1994**, *90*, 2865-2871.
32. E. Hückel, *Z. Phys.*, **1931**, *70*, 204.
33. M. V. Diudea, T. S. Balaban, E. C. Kirby, and A. Graovac, *Phys. Chem*. *Chem. Phys*, **2003**, in press.
34. M. Yoshida, M. Fujita, P. W. Fowler and E. C. Kirby, *J. Chem. Soc., Faraday Trans*., **1997**, *93*, 1037-1043.
35. M. V. Diudea, O. Ursu, and C. L. Nagy, “Babes-Bolyai" University, **2002**.
36. M. V. Diudea and M. Stefu, “Babes-Bolyai" University, **2002**.
37. M. Goldberg, *Tôhoku Math. J*., **1937**, *43*, 104-108.
38. M. Dutour and M. Deza, LIGA, ENS/CNRS, Paris, **2003** (preprint).